



Published in final edited form as:

Clin Cancer Res. 2013 December 15; 19(24): . doi:10.1158/1078-0432.CCR-13-0621.

HAb18G/CD147 Promotes pSTAT3-Mediated Pancreatic Cancer Development via CD44s †, ‡

Ling Li^{1,2,*}, Wenhua Tang^{1,3,*}, Xiaoqing Wu^{1,3,*}, David Karnak¹, Xiaojie Meng^{1,3}, Rachel Thompson¹, Xinbao Hao^{1,4}, Yongmin Li¹, Xiaotan T. Qiao⁵, Jiayuh Lin⁶, James Fuchs⁷, Diane M. Simeone⁸, Zhi-Nan Chen^{2,§}, Theodore S. Lawrence¹, and Liang Xu^{1,3,§}

¹Department of Radiation Oncology, University of Michigan Medical Center, Ann Arbor, MI; USA

²Cell Engineering Research Centre and Department of Cell Biology, State Key Laboratory of Cancer Biology, Fourth Military Medical University, Xi'an, China

³Departments of Molecular Biosciences and Radiation Oncology, University of Kansas, Lawrence, KS, USA

⁴Department of Hematology/Oncology, Hainan University Medical School, Haikou, Hainan, China

⁵Department of Cell and Developmental Biology, University of Michigan, Ann Arbor, MI, USA

⁶Department of Pediatrics, College of Medicine, Ohio State University, Columbus, OH, USA

⁷Division of Medicinal Chemistry and Pharmacognosy, College of Pharmacy, Ohio State University, Columbus, Ohio, USA

⁸Department of Surgery, University of Michigan Medical Center, Ann Arbor, MI, USA

Abstract

Purpose—STAT3 plays a critical role in initiation and progression of pancreatic cancer. However, therapeutically targeting STAT3 is failure in clinic. We previously identified HAb18G/CD147 as an effective target for cancer treatment. In this study, we aimed to investigate potential role of HAb18G/CD147 in STAT3-involved pancreatic tumorigenesis *in vitro* and *in vivo*.

Experimental Design—The expression of HAb18G/CD147, pSTAT3 and CD44s were determined in tissue microarrays. The tumorigenic function and molecular signaling mechanism of HAb18G/CD147 was assessed by *in vitro* cellular and clonogenic growth, reporter assay, immunoblot, immunofluorescence staining, immunoprecipitation, and *in vivo* tumor formation using loss or gain-of-function strategies.

Results—Highly expressed HAb18G/CD147 promoted cellular and clonogenic growth *in vitro* and tumorigenicity *in vivo*. CyPA, a ligand of CD147, stimulated STAT3 phosphorylation and its downstream genes cyclin D1/survivin through HAb18G/CD147 dependent mechanisms. HAb18G/

†Sources of Support: This work was supported in part by U.S. National Institutes of Health grants R01 CA121830 S1 (to L.X.), R01 CA134655 (to L.X.), and 5P30 CA46592 (University of Michigan Cancer Center Support Grant), Kansas Bioscience Authority Rising Star Award (to L.X.), and China National Science and Technology Major Project 2013ZX09301301 (to Z.N.C.) and National Basic Research Program 2009CB521704 (to Z.N.C.).

‡Author disclosures: The authors declare no conflicts of interest.

§To whom correspondence and requests for reprints should be addressed: Liang Xu, M.D., Ph.D., Departments of Molecular Biosciences and Radiation, University of Kansas, 4002 Haworth Hall, 1200 Sunnyside Avenue, Lawrence, KS 66045, USA. Phone: 785-864-5849, Fax: 785-864-1442, xul@ku.edu; or Zhi-Nan Chen, M.D., Ph.D., Cell Engineering Research Centre and Department of Cell Biology, State Key Laboratory of Cancer Biology, Fourth Military Medical University, Xi'an, Shanxi 710032, China. Phone: 86-29-83293906, Fax: 86-29-83293906, znchen@fmmu.edu.cn.

*Equal contribution

CD147 was associated and co-localized with cancer stem cell marker CD44s in lipid rafts. The inhibitors of STAT3 and survivin, as well as CD44s neutralizing antibodies suppressed the HAb18G/CD147-induced cell growth. High HAb18G/CD147 expression in pancreatic cancer was significantly correlated with the poor tumor differentiation, and the high co-expression of HAb18G/CD147-CD44s-STAT3 associated with poor survival of patients with pancreatic cancer.

Conclusions—We identified HAb18G/CD147 as a novel upstream activator of STAT3 via interacts with CD44s and plays a critical role in the development of pancreatic cancer. The data suggest HAb18G/CD147 could be a promising therapeutic target for highly aggressive pancreatic cancer and a surrogate marker in the STAT3-targeted molecular therapies.

Keywords

Pancreatic cancer; HAb18G/CD147; CD44; STAT3; tumor development

Introduction

Pancreatic ductal adenocarcinoma (PDCA) remains a devastating and almost uniformly lethal disease with the 5-year survival less than 5% (1, 2). Most patients with advanced unresectable PDCA either do not respond, or respond transiently and modestly to systemic chemo/radiotherapy (3, 4). This dire clinical situation cries for our deep understanding of the genetics and biology of PDCA and our efforts on identifying novel therapeutic approaches.

It has been widely accepted that PDCA arise from K-ras mutations, followed by acquisition of additional epigenetic and genetic somatic alterations, including inactivation or point mutation of *p16/CDKN2A*, *TP53*, and *DPC4/SMAD4* (2, 5). However, the above genetic information has not yet led to the development of effective targeted therapeutic strategies.

Signal transducer and activator of transcription 3 (STAT3) integrates signals from cytokines and growth factors into transcriptional responses in target cells. It is an important regulator of stem cell self-renewal, cancer cell survival and inflammation (2, 6, 7). It was recently reported that STAT3 has critical roles in the development of PDCA, especially the initiation and progression of PDCA by controlling expression of target genes survivin, cyclin D1 and matrix metalloproteinase 7 (MMP7) (5, 8, 9). In the context of acute pancreatitis and K-ras induced pancreatic intraepithelial neoplasias (PanINs) lesions, STAT3 mediated tumor initiation are related to its ability to promote cell survival and proliferation, and to induce reprogramming of normal pancreatic epithelial cells into progenitor-like phenotype, a process assuming a proneoplastic fate (5, 8).

In addition, constitutive activation of STAT3 is frequently detected in pancreatic cancer and has been associated with a poor prognosis, and served as a therapeutic target (10). Due to lack of enzyme activity, targeting STAT3 is not easy. Inhibition of STAT3 phosphorylation/activation using monoclonal antibody or small molecules that antagonize growth factor and cytokine receptor show modest efficacy of treatment of pancreatic cancer and develop resistance finally (10). Since multiple factors can activate STAT3, blockade of a single molecule related to STAT3 activation may not sufficiently abrogate STAT3. Therefore, a novel upstream signaling molecule responsible for STAT3 activation would give further insight into the mechanisms on how STAT3 contributes to PDCA tumorigenesis. Such molecules may be useful for tailoring cancer treatment when targeting STAT3.

HAb18G/CD147, which belongs to the CD147 (also called EMMPRIN or basigin) family, is a transmembrane protein identified by screening a human hepatocellular carcinoma (HCC) cDNA library using a monoclonal antibody HAb18 in our laboratory (11). HAb18G/CD147 is capable of promoting tumor invasion and metastasis via inducing MMP production (12)

and cell motility (13), and affecting tumor cell angiogenesis (14), chemoresistance (15) and glycolysis (16). Due to its high expression in many carcinomas, HAb18G/CD147 acts as a cancer-associated biomarker for detection (17) and an effective target for treatment (18). Licartin, a ¹³¹I-labeled antibody HAb18 F(ab')₂ against HAb18G/CD147 has been used to treat primary HCC and prevent tumor recurrence of post liver transplantation in advanced HCC patients in China (19, 20). These results suggest that HAb18G/CD147 play an important role in cancer metastasis and progression. Recently, we showed that HAb18G/CD147 promote epithelial-mesenchymal transition (21), anoikis resistance and anchorage-independent growth *in vitro* (22, 23) and tumorigenic potential of liver cancer *in vivo* (21), indicating a possible role of HAb18G/CD147 in tumor initiation.

Nevertheless, the function of HAb18G/CD147 has not yet been fully understood in pancreatic cancer. Highly expressed CD147 has been reported in human PDCA tissues and cell lines (24–26), these studies either, however, have a relatively small sample size of patients (e.g. 39–55 cases), or are lack of a clinicopathologic data. We also showed that HAb18G/CD147 was highly expressed in breast carcinomas and sarcomas (17), but its expression in pancreatic cancers were not included in that analysis. Although targeting CD147 by siRNA (27, 28) or monoclonal antibody (29, 30) can reduce cell growth and invasion *in vitro* and inhibits tumor growth and metastasis in a xenograft model, the role of HAb18G/CD147 in the early promotion of PDCA, especially in STAT3-involved PDCA initiation, remains largely unknown.

To explore the potential molecular targets of HAb18G/CD147, we searched the oncomine database for genes co-expressed with CD147 in pancreas (31). We observed that CD147 highly expressed in primary pancreatic cancer patients (32–34), and STAT3 is among the top listed genes that highly correlated with CD147 (Figure S1). It has been reported that CyPA, as a CD147 ligand, promotes pancreatic cancer cell growth (35, 36), and contributes to STAT3-mediated cell survival (37). These evidences promote us to investigate the role of HAb18G/CD147 in STAT3-mediated cell growth signaling using CyPA as a stimulus of HAb18G/CD147 activation. Typically, CD147 transmits extracellular signal by forming complexes with another membrane protein upon CyPA stimulation (38); while activated STAT3 promotes the transcription of target genes by phosphorylating and translocation from cytoplasm into nucleus. CD44 (CD44 v3–10) has been reported to activate STAT3 signaling (39), and co-localize with CD147 in cancer cells (40, 41), suggesting a potential role of CD44 in the CyPA-HAb18G/CD147-STAT3 mediated cell growth signaling in pancreatic tumorigenesis.

Here, we perform a systematic study to investigate the relationship among HAb18G/CD147, CD44 and STAT3 in the development of pancreatic cancer. We identified HAb18G/CD147 interacting with CD44s as a novel upstream activator of STAT3 signaling, which plays a critical role in the development of pancreatic cancer. Our data suggest that HAb18G/CD147 could be a promising therapeutic target for highly aggressive pancreatic cancer and a surrogate marker for the STAT3-targeted molecular therapies.

Materials and Methods

Antibodies and reagents

Antibodies to phospho-STAT3 (Tyr⁷⁰⁵) and total STAT3 were purchased from Cell Signaling (Danvers, MA), CD44s clone MEM-263 from Abnova (Walnut, CA), survivin from Novus (Littleton, CO), cyclin D1 and α -tubulin from Santa Cruz (Santa Cruz, CA), goat anti-rabbit Texas-Red and goat anti-mouse FITC from Jackson ImmunoResearch (West Grove, PA), GFP, β -actin, goat anti-rabbit horseradish peroxidase (HRP), goat anti-mouse HRP, mouse IgG, cholera toxin subunit B conjugates CTB-594 and geneticin (G418) from

Invitrogen (Carlsbad, CA). Anti-mouse CD44s antibody H4C4 was obtained from the University of Iowa Developmental Studies Hybridoma Bank, and anti-mouse HAB18G/CD147 antibody HAB18 was prepared as reported (20). Recombinant human CyPA, cycloheximide (CHX) and doxycycline (DOX) were purchased from Sigma. Puromycin and YM-155 were purchased from InvivoGen and Active Biochem, respectively. FLLL32 were prepared as previously described (42).

Cell lines and constructs

Human pancreatic cancer cell lines and normal human embryonic lung fibroblast cell line WI-38 and embryonic kidney cell line HEK293 were obtained from the American Type Culture Collection (ATCC) and cultured in DMEM (HyClone), supplemented with 10% fetal bovine serum (HyClone). All cell lines from ATCC have been tested and authenticated with genotyping by ATCC and used within 6 months after receipt. The pGIPZ and pTRIPZ empty vector, CD147 pLKO.1, pGIPZ and pTRIPZ lentiviral shRNA constructs were obtained from Open Biosystems. The MISSION® Non-Target shRNA Control Vector (pLKO.1-NTC) was obtained from Sigma. Human CD147 cDNA was subcloned into the pEGFP-N1 expression vector (Clontech) as described (43). CD44s siRNA and control siRNA were obtained from Dharmacon. The survivin lentiviral shRNA and empty vector were obtained from OriGene. The reporter plasmid pSTAT3-luc and a pGL3-Control Vector were purchased from Promega.

Patient samples

Fresh and paraffin-blocked pancreatic tumor and adjacent non-tumor tissues from pancreatic cancer patients were obtained from University of Michigan Comprehensive Cancer Center (UMCCC) Histology Core according to an IRB-approved human protocol (H7094) and from National Engineering Center for Biochip according to an approved human protocol. Tissue microarrays (TMAs) from 193 patients were obtained from UMCCC Histology Core for analyzing HAB18G/CD147 expression in the progress of pancreatic tumorigenesis. They were constructed by two different recipient paraffin blocks: “control tissue array” and “tumor tissue array”. The “control tissue array” included 53 cases of normal pancreatic tissues and 7 cases of pancreatitis; the “tumor tissue array” included 2 cases of pancreatic intraepithelial neoplasia (PanIns), 6 cases of cystadenoma, 17 cases of intraductal papillary mucinous neoplasm (IPMN) and 108 cases of PDCA.

For analysis of the association of HAB18G/CD147 expression with clinic-pathologic parameters, TMA of 157 pairs of pancreatic cancer tissue and adjacent non-tumor tissues (within the cancer edge of 5 cm) were obtained from NECB. The clinical, pathological, and treatment information, together with follow-ups and forms of consents were also obtained for these 157 patients.

Establishment of stable cell lines

The CD147 lentiviral shRNA or control shRNA was introduced into cells using FuGene6 (Roche), while CD147/EGFP cDNA and pEGFP control vector was transfected with HEK293 cells using Lipofectamine 2000 (Invitrogen). Knock-down or knock-in cells was selected by adding 4–6 µg/ml of puromycin or 1 mg/ml of G418 to the culture medium, and expression of inducible shRNA was induced in the presence of 1µg/ml doxycycline. Silencing or increase of HAB18G/CD147 expression was verified by qRT-PCR and immunoblot analysis.

Cell growth assay

Cells were plated in 24-well plates and were counted every 24 hours for 3–5 days using a haemocytometer, or measuring WST-8 dye absorbance at 570nm. A cell growth curve was drawn according to the cells number with the specified incubation time. For growth inhibition of STAT3/survivin inhibitor or CD44s antibody, cells were serum-starved for 24 hours before adding 5 $\mu\text{mol/L}$ FLLL32 or 0.05–0.1 $\mu\text{mol/L}$ YM155 or 10 $\mu\text{g/ml}$ H4C4 or nIG for one hour followed by 72–96 hour 100nmol/L CyPA treatment. The results are shown as relative cell growth inhibition, which normalized to their individual control.

Colony formation assay

Cells were cultured in DMEM containing 10% FBS with 250 cells in each 6-well plate. Plates were maintained at 37°C in a humidified incubator for 7–10 days. The colonies was stained by 0.1% crystal violet and calculated under microscopy.

In Vitro Matrigel Invasion Assay

Cells were seeded into upper chambers of 8 μm pore transwells coated with matrigel and then allowed to invade the matrigel for 36 hours. Invaded cells were stained with Diff-Quik™ stain (Allegiance), and the invasive potential of the cells was determined by counting the number of cells that had invaded to the lower surface of the filter in 10 different areas under an inverted light microscope (Olympus BX41).

STAT3 reporter assay

Cells were seeded in 48-well plates and were then transfected with 0.5 μg STAT3-luc reporter constructs or 0.5 μg of a GL3 vector control using Lipofectamine 2000. Sixteen hours after transfection, cells were treated with CyPA for 18 hours. Luciferase activity was then measured in cell lysates by a POLARstar OPTIMA Microplate Reader using the Bright-Glo™ Luciferase Assay System (Promega) according to the manufacturer's protocol. For comparison, luciferase activity was normalized to β -galactosidase expression using the Beta-Glo® Assay System (Promega).

Animal studies

Animal studies of tumor formation and tumor growth were performed as described previously (44). Briefly, 1×10^6 cells in 0.2 ml DMEM inoculated into five- to six-week old female athymic NCr-nu/nu nude mice subcutaneously (s.c.) on both flanks. Five mice with 2 injection sites (up and down) on each mouse were used for each type of construct (n=10 per group). The tumor sizes and animal body weights were measured twice weekly and plotted. Tumor volume was calculated using the formula: $(\text{length} \times \text{width}^2)/2$. All animal experiments were performed according to the protocol approved by the University of Michigan Animal Care and Use Committee and in accordance with NIH guidelines.

Quantitative real-time RT-PCR (qRT-PCR)

Total RNA extraction and cDNA synthesis were carried out as previously described (45). qRT-PCR was carried out using an ABI 7700® real-time PCR system (Applied Biosystems) with gene specific primers for HAb18G/CD147, CD44, STAT3, CyclindD1, survivin, MMP1, MMP2, MMP9, β actin, GAPDH or 18sRNA (Supplementary Table 1). Individual genes of interest (GOI) in were normalized to housekeeping genes (HKG): β -actin, 18sRNA or GAPDH. Relative mRNA levels are presented as unit values of $2^{-\Delta\text{Ct}} = 2^{-(\text{Ct}(\text{HKG}) - \text{Ct}(\text{GOI}))}$.

Immunohistochemistry

TMA staining was performed by standard immunohistochemistry procedures. To confirm the specificity of the primary antibodies, tissue sections were incubated in the absence of the primary antibodies and with control mouse IgG. The number of positively stained cells and the intensity of positive staining on epithelium and stromal cells were independently scored by 2 pathologists in a blinded manner. The percentage of positive stained cells was scored as: 0, 1–25%, 26–75% and > 75%. The intensity of positive immunostaining on the cells was graded by an experienced pancreatic pathologist in a blinded manner and classified into four categories: 0, 1, 2, and 3 representing no visible staining; light brown, mid-brown and dark brown staining, respectively, with the same intensity covering more than 75% of the staining area. For statistical analysis, the stained tumor tissues were divided into two groups: the low-expression group and the high-expression group. For membranous HAb18G/CD147, only 3+ specimens were defined as high expression; for membranous CD44s and phospho-STAT3-positive nuclei, the samples with 1+ staining >50% of cells or 2+ staining in >20% or all 3+ staining of cells were defined as high expression.

Immunofluorescence staining

Cells grown on chambered cover slips were either left untreated or treated with 100nM CyPA for 30 minutes. After fixedness, cells were blocked and probed with anti-HAb18G/CD147 antibody HAb18 and anti-CD44s antibody H4C4, and were then detected with fluorochrome-conjugated FITC, Texas-Red or CTB594. Cover slips were counterstained with 4',6-diamidino-2-phenylindole (DAPI, Invitrogen) for visualization of nuclei. Cell images were observed under a fluorescent microscope (Olympus).

Immunoblot and Immunoprecipitation assay

Immunoblot assay were performed using standard methods (45). Cells were treated with CyPA and/or H4C4 and/or mouse IgG as required in each assay. Membranes were probed with total and phosphorylated antibodies as detailed above in materials. Immunoprecipitation assays were performed using the Pierce[®] Co-Immunoprecipitation (Co-IP) Kit (Thermo Fisher Scientific) according to the manufacturer's instructions with minor modifications (45). We used 25 µg of each monoclonal antibody (complete IgG molecule) specific to either HAb18G/CD147 (HAb18) or CD44s (H4C4) for immobilization. A mouse IgG1 isotype antibody (Sigma-Aldrich) served as a negative control. Adsorbed immune complexes were washed, eluted and then subjected to immunoblot analysis using HAb18 and H4C4.

Statistical analysis

All data shown are mean ± SEM of triplicate values from three separate experiments. * $P < 0.05$, ** $P < 0.01$ and *** $P < 0.001$ as compared with the control group. Independent Student t tests or One-way ANOVA was used to compare the continuous variables between the 2 groups or more than 2 groups, and categorical variables were compared using the χ^2 test. Spearman rank correlation was conducted to analyze expression correlations among HAb18G/CD147 and CD44s. The Kaplan-Meier method and the log-rank test were used to compare overall survival, defined as the time of patients from surgery until death (patients alive were censored at the time of their last follow-up). Statistical analyses were carried out with statistical analysis software program SPSS 13.0 software (IBM) and Prism 5.0 software (GraphPad).

Results

HAb18G/CD147 is highly expressed in pancreatic cancer cell lines

To determine how HAb18G/CD147 contributes to pancreatic tumor development, we firstly determined the HAb18G/CD147 expression in a panel of pancreatic cancer cell lines, a human pancreatic cancer primary tumor early-passage xenograft (J2) and immortalized human pancreatic epithelial cell HPDE, as well as normal human embryonic lung fibroblast cell line WI-38 and embryonic kidney cell line HEK293. HAb18G/CD147 mRNA and protein expression were significantly higher in pancreatic cancer cell lines and HPDE than that in WI-38 and HEK293 cells (Figure S2). Based on the cells' endogenous HAb18G/CD147 expression and capacity for tumor formation (44), we selected PANC-1 and MIA PaCa-2 cells for further knock-down studies and HEK293 with low endogenous HAb18G/CD147 expression for knock-in studies.

HAb18G/CD147 promotes cellular and clonogenic growth *in vitro* and tumor formation *in vivo*

To determine the potential biological function of HAb18G/CD147 in pancreatic cancer, we adopted a loss-of-function strategy using three different lentiviral vectors: untagged pLKO CD147-shRNA targeting the coding region, a GFP tagged pGIPZ CD147-shRNA targeting the coding regions and the 3'UTR, and an RFP tagged inducible pTRIPZ CD147-shRNA targeting the coding regions and the 3'UTR. We also adopted a gain-of-function strategy to knock-in HAb18G/CD147 cDNA into HEK293 cells.

When HAb18G/CD147 expression was effectively silenced (typically 60–80% reduction of the total (Figure S3D, Table S5), which functionally validated by decrease of cell invasion (Figure S3), cellular and clonogenic growth was significantly decreased (Figure 1A, 1B). In contrast, HAb18G/CD147 knock-in HEK293 cells with significantly increased HAb18G/CD147 expression (6.32-fold increases in mRNA levels and >3-fold increases in protein levels, comparable to the average expression in pancreatic cancer cells), have a significantly increased cell invasion (Figure S3) and cellular and clonogenic growth (Figure 1A, 1B). These results were confirmed with pGIPZ-CD147 shRNA and pTRIPZ inducible CD147 shRNA (Figure S4A, S4B).

Next, we examined the effects of HAb18G/CD147 on tumor formation in a xenograft mouse model. After knockdown of HAb18G/CD147, both tumor formation and tumor growth were significantly decreased, with a 71.8%–87.9% reduction in tumor sizes (n=10, Figure 1C, 1D, S4C). These results were confirmed in MIA PaCa-2 xenograft mouse model using pGIPZ CD147 shRNA (Figure S4D). Conversely, HAb18G/CD147 knock-in promoted tumorigenicity indicated by a significantly increased tumor incidence (10/10 vs. 2/10, $P < 0.001$, n=10, Figure 1C) and tumor volume (793.9 ± 549.3 vs. 110.1 ± 5.8 , Figure 1D, S4C) in HEK293 xenograft model. These data suggest that highly expressed HAb18G/CD147 is associated with high tumorigenicity of pancreatic cancer cells, thus support the potential role of HAb18G/CD147 in promoting pancreatic tumor development.

HAb18G/CD147 is involved in the STAT3 signaling pathway

We first determined the effects of CyPA, a natural ligand of HAb18G/CD147, on the pancreatic cancer cell growth as well as its effect on the modulation of HAb18G/CD147, STAT3 and the downstream genes cyclin D1 and survivin. We observed that CyPA induced HAb18G/CD147 protein expression in a dose- and time-dependent manner (Figure S5). The protein levels of pSTAT3⁷⁰⁵ and its targets cyclin D1/survivin were also increased in a dose- and time- depended manner upon CyPA treatment (Figure S5).

Next, we determined whether or not these effects are HAb18G/CD147 dependent by knock-down or knock-in of HAb18G/CD147. STAT3 mRNA levels were not significantly changed (Figure 2A) but the CyPA-induced pSTAT3 and cyclin D1/survivin protein expression were attenuated after knock-down of HAb18G/CD147 (Figure 2B, *left*), supporting that the CyPA increased protein expression of pSTAT3/cyclin D1/survivin through HAb18G/CD147-dependent mechanism. In addition, the mRNA levels of cyclin D1 and survivin were significantly decreased by knock-down of HAb18G/CD147 in PANC-1 cells with low pSTAT3 signaling, whereas they were only slightly changed in MIA PaCa-2 cells with high pSTAT3 (Figure 2A, S2D), supporting that HAb18G/CD147 promoted transcription of cyclin D1/survivin in a pSTAT3-dependent manner. These results were further confirmed by knock-down of HAb18G/CD147 using pTRIPZ inducible CD147-shRNA (Figure 2B, *right*). In contrast, STAT3, cyclin D1 and survivin protein levels were significantly increased by knock-in of HAb18G/CD147 in HEK293 cells (Figure 2B, *left*). Taken together, the regulation of CD147 on STAT3 appears not at the mRNA level, but at STAT3 phosphorylation. The observed colony formation inhibition by HAb18G/CD147 may be due to the decrease of pSTAT3 levels, and this effect is cell line dependent. As MIA PaCa-2 has more pSTAT3 than PANC-1, more clonogenic inhibition was observed in the MIA PaCa-2 clones with HAb18G/CD147 shRNA as compared with that in the PANC-1 clones.

Furthermore, the reporter assay showed that STAT3 transcriptional activity was significantly affected upon HAb18G/CD147 knock-down or knock-in (Figure 2C), but no significant changes upon CyPA stimulation (data not shown). These results suggested that HAb18G/CD147 served as an upstream activator of STAT3 signaling in pancreatic cancer cells, and that HAb18G/CD147 might be more important than CyPA in STAT3 activation.

To evaluate whether STAT3 and survivin are involved in the CyPA-HAb18G/CD147 induced cell growth, we performed cell growth assay for MIA PaCa-2 cells by exposure to CyPA and either STAT3 inhibitor FLLL32/WP1066 or survivin inhibitor YM155. We observed that FLLL32/WP1066 and YM155 significantly inhibited CyPA-induced cell growth (Figure 2D, S5F), and CyPA rescued the inhibition of cell growth by survivin shRNA (Figure 3A). Furthermore, the cell growth inhibition ratio of WP1066 increased up to 2 folds by knock-down of HAb18G/CD147 (Figure 3B). These data suggest that the STAT3 and its downstream gene survivin play an important role in CyPA-HAb18G/CD147-mediated cell growth.

CD44s is involved in the activation of STAT3 by HAb18G/CD147 in lipid rafts

As shown in Figure 3C–D, CD44s siRNA and CD44s antibody H4C4 abolished the CyPA-induced STAT3 phosphorylation and down-stream signaling, indicating that CD44s is required for CyPA-HAb18G/CD147 mediated STAT3 transcription activation. CD44s protein, but not mRNA, levels were significantly affected upon CyPA stimulation (Figure S5D) or HAb18G/CD147 knock-in (Figure S6A, S6B), indicating that transcriptional regulation may not be the clue that connects HAb18G/CD147 with CD44s. Our IP assay showed that HAb18G/CD147 and CD44s were co-localized and significantly associated in the untreated cells (Figure 4A, 4B). This association was much stronger in the HAb18G/CD147 knock-in HEK293/CD147 cells than that in HAb18G/CD147 knock-down MIA PaCa-2/A6 cells, and both were enhanced further upon CyPA stimulation. By immunofluorescence staining, we observed that both HAb18G/CD147 and CD44s were evenly located on the cell membrane before treatment, but were translocated to the GM1-enriched lipid rafts (identified by CTB-594 staining) after CyPA stimulation (Figure 4C, S6C). However, this translocation of CD44s in the lipid rafts was blocked after knocking down HAb18G/CD147. These results suggest that HAb18G/CD147 may co-localize and

form a signaling complex with CD44s in the lipid rafts, and CyPA stimulation, though not a prerequisite, may promote the association of the two proteins.

Furthermore, we observed that the CD44s blocking antibody H4C4 attenuated the CyPA-induced cell growth to the level of the IgG control, and decreased the level of EGFR but not HAb18G/CD147 (Figure 4D, 3D). These data indicates that HAb18G/CD147 promotes pSTAT3-mediated cell growth through CD44s.

HAb18G/CD147, CD44s and STAT3 are highly expressed in human pancreatic cancer and correlate with pancreatic cancer patients' survival

We found that HAb18G/CD147 mRNA levels in human pancreatic tumor tissues are significantly higher (average 4.27-fold) than that in the adjacent normal tissues (Figure 5A). In a TMA with 193 pancreatic tissues, HAb18G/CD147 is highly expressed in only 22.6% and 14.3% of normal pancreatic tissue and chronic pancreatitis respectively, but in 56% and 55.6% of pancreatic preneoplasma and PDCA, respectively (Figure 5B, Table 1).

We next investigated the correlation between HAb18G/CD147 expression and clinicopathological parameters in 157 cases of pancreatic cancer (Table S2). No significant correlation exists in age, gender, tumor type, size and location, AJCC stage and patient survival. But high HAb18G/CD147 expression seems have more lymph node invasion (52.94% vs. 42.59%) and advanced TNM stage (51.35% vs. 37.5%). Moreover, high HAb18G/CD147 expression was found to be significantly associated with a poor tumor differentiation (51.43% vs. 15.65%, $P < 0.0001$). Taken together, being up-regulated in both pancreatic preneoplasma and PDCA, and being correlated to poor tumor differentiation and advanced TNM stage, HAb18G/CD147 may have a role in pancreatic tumor development.

To investigate whether HAb18G/CD147-mediated tumor growth and CD44s-pSTAT3 expression are associated in patient samples, we analyzed the co-expression of CD44s-pSTAT3 with HAb18G/CD147 in 157 pancreatic cancer tissues. As indicated, high HAb18G/CD147 expression was significantly correlated with high CD44s expression (Spearman $r = 0.4961$, $P < 0.001$, Figure S6D, S6E), but not with high pSTAT3 nuclear positivity (Table 2). With regard to the clinical pathological factors, patients with high expression of HAb18G/CD147 and CD44s had poor tumor differentiation ($P < 0.0001$, Table S3) and a lower median survival, as compared to patients with low expression of HAb18G/CD147 and CD44s, although the latter lacks statistical difference ($P = 0.311$, Figure 5C, *up*).

Moreover, patients with high expression of all three genes had a higher incidence of poor tumor differentiation (60.87% vs. 7.69%, $P = 0.002$) and mortality (60% vs. 28.57%, $P = 0.218$), as well as a 75% survival of 4 months, as compared with that of 10 months for patients with low expression of the three genes (hazard ratio [HR] of death = 3.024, 95% confidence interval [CI] = 0.642 to 15.983, $P = 0.12$) (Table S4, Figure 5C). These results suggest that HAb18G/CD147-CD44s-pSTAT3 association might be used as a prognosis marker for pancreatic cancer.

Discussion

In this study, we found that HAb18G/CD147 was highly expressed in pancreatic cancer cell lines, chronic pancreatitis, preneoplasma and PDCA. Knockdown of HAb18G/CD147 significantly inhibited the tumor cell invasion, cellular and clonogenic growth *in vitro* and reduced tumor formation and tumor growth in xenograft mouse model. Moreover, we showed that HAb18G/CD147 and CD44s are involved in the activation of STAT3 signaling pathway. Finally, we demonstrated that patients with high expression of HAb18G/CD147,

CD44s, and pSTAT3 had higher mortality and poorer tumor differentiation, and poorer survival, as compared to the patients with low expression of these three genes. These data support that HAB18G/CD147 plays a novel oncogenic role in pancreatic tumor development, besides its well-known role in regulating MMP-related metastasis.

We previously showed that HAB18G/CD147 play an important role in liver tumor metastasis under different experimental and clinical conditions (13, 20). In this study, we showed that HAB18G/CD147 plays a role in early promotion of pancreatic cancer. HAB18G/CD147 antibody has been used in clinical practice for liver cancer therapy, and other CD147 antibodies are in preclinical development for pancreatic cancer (29, 30, 46), suggesting the potential clinical application of HAB18G/CD147 antibody for PDCA patient.

Both HAB18G/CD147 activator CyPA and STAT3 were related to inflammation and cancer, suggesting a potential link between inflammation and pancreatic tumor initiation via CyPA-HAB18G/CD147-STAT3 signaling. STAT3, as a mediator of inflammation-associated processes, plays a critical role in PDCA initiation and progression and has been under active investigation as a potential target for PDCA therapy (5, 8, 9). However, STAT3-targeted anticancer drug, either anti-EGFR antibodies or small-molecule tyrosine kinase inhibitors, only showed a limited efficacy (10). As STAT3 occupies a point of convergence for many signaling pathways, blockade of existed upstream signaling to STAT3 activation may not sufficiently abrogate STAT3. In this study, we showed that CyPA induced STAT3 phosphorylation through HAB18G/CD147 dependent mechanism, suggesting that HAB18G/CD147 is a real upstream regulator of STAT3 activation. Pancreatic cancer cells with high HAB18G/CD147 levels and/or activity had higher active STAT3 signaling, on which the cells depend for survival and proliferation, much like the so-called “oncogene addiction”. Actually, CyPA has previously been reported to regulate STAT3 tyrosine phosphorylation and nuclear translocation (37). We also showed that HAB18G/CD147 promotes tumor growth by regulating the expression of survivin and cyclin D1. This result is in consistent with previous reports that STAT3 promotes tumor early promotion by controlling the transcription of anti-apoptotic gene survivin and proliferative gene cyclin D1 (8). These data suggest that HAB18G/CD147 may exert its tumor-promoting function by activating the STAT3 phosphorylation, indicating a novel role for HAB18G/CD147 in the STAT3-mediated tumor early promotion in PDCA. It has been reported that the expression of EMMPRIN (CD147) may be modulated by STAT3 ODN (47), indicating a positive feedback loop between HAB18G/CD147 and STAT3. In other word, CyPA-HAB18G/CD147 activates STAT3 phosphorylation, and then pSTAT3 promote HAB18G/CD147 transcription. Thus, the CyPA-HAB18G/CD147-STAT3 mediated growth-promoting signaling could be amplified, in which case STAT3 inhibitors may have better effects for cancer cells with high expression of HAB18G/CD147. In a rationally designed clinical trial of STAT3-targeted cancer therapy, the HAB18G/CD147 level in cancer patients should also be considered. This will help us to select a patient subgroup that is more likely to respond to the molecularly targeted therapy. HAB18G/CD147 may thus become an important surrogate marker in clinical trials of molecular therapies targeting STAT3.

HAB18G/CD147 expression is highly correlated with CD44s expression in our analysis. Patients with HAB18G/CD147^{high}/CD44s^{high}/ pSTAT3^{high} co-expression show high mortality, implying a potential link of HAB18G/CD147 to tumor initiation by associating with the cancer stem cell (CSC) marker CD44s (48, 49), and by regulating the CSC signaling molecule STAT3 (50). CD147 has been shown a propensity to form complexes with membrane proteins like MCT, CD98, caveolin, integrins, basigin-2 (CD147) and basigin-3, thereby shielding the charge in an energetically stable state (18, 38, 43). We show that HAB18G/CD147 forms a signaling complex with CD44s, and CD44s may mediate part of the oncogenic activities of HAB18G/CD147 by activating the STAT3 signaling. The co-

localization and co-expression of CD147 and CD44 has been reported in breast and prostate cancer (40, 41, 51), our data provide new evidence of functional link and clinical relevance between them in pancreatic cancer. The HAb18G/CD147 interaction with CD44s, but not CD44v, plays a role in pancreatic tumor development. Furthermore, HAb18G/CD147 and CD44s distribute together in the specific signaling platform, lipid rafts, which facilitate efficient downstream signal transduction. As the distribution and activity of CD44s depend on CyPA-HAb18G/CD147, consistent with a previous report that HAb18G/CD147 membrane localization is not affected by hyaluronan oligomers that antagonize the hyaluronan-CD44 interaction (51). Therefore, we propose that upon CyPA stimulation, HAb18G/CD147 first clusters and recruits CD44s in the lipid rafts to form a signaling complex, and then promotes STAT3 phosphorylation and cyclin D1/survivin transcription, finally leads to cell survival and cell cycle progression (Figure 5D).

In conclusion, our study suggests that HAb18G/CD147 is a novel upstream activator in STAT3-mediated pancreatic tumor development by forming signaling complex with the CSC marker CD44s, and that co-expression of HAb18G/CD147-CD44s-STAT3 indicates poor prognosis in patients with pancreatic cancer. This information will be valuable for a better understanding of the relationship between inflammation and pancreatic cancer initiation and progression induced by STAT3; in addition, our results establish HAb18G/CD147 as a novel therapeutic target for highly aggressive pancreatic cancer and as a surrogate marker in clinical trials of molecular therapies targeting STAT3.

Supplementary Material

Refer to Web version on PubMed Central for supplementary material.

Acknowledgments

We thank Dr. Susan Harris for help with editing of the manuscript; Dr. Thomas Giodano, Dr. Dafydd Thomas and Ms. Michelle Vinco in the UMCCC Tissue Core for providing tissues and tissue microarrays and help on immunohistology staining. We also thank the UMCCC Unit of Laboratory Animal Medicine (ULAM) for their help with the animal experiments.

References

1. Jemal A, Siegel R, Xu J, Ward E. Cancer statistics, 2010. *CA Cancer J Clin.* 2010; 60:277–300. [PubMed: 20610543]
2. Perez-Mancera PA, Guerra C, Barbacid M, Tuveson DA. What we have learned about pancreatic cancer from mouse models. *Gastroenterology.* 2012; 142:1079–92. [PubMed: 22406637]
3. Conroy T, Desseigne F, Ychou M, Bouche O, Guimbaud R, Becouarn Y, et al. FOLFIRINOX versus gemcitabine for metastatic pancreatic cancer. *N Engl J Med.* 2011; 364:1817–25. [PubMed: 21561347]
4. Kim R. FOLFIRINOX: a new standard treatment for advanced pancreatic cancer? *Lancet Oncol.* 2011; 12:8–9. [PubMed: 21050812]
5. Corcoran RB, Contino G, Deshpande V, Tzatsos A, Conrad C, Benes CH, et al. STAT3 plays a critical role in KRAS-induced pancreatic tumorigenesis. *Cancer Res.* 2011; 71:5020–9. [PubMed: 21586612]
6. Li N, Grivennikov SI, Karin M. The unholy trinity: inflammation, cytokines, and STAT3 shape the cancer microenvironment. *Cancer Cell.* 2011; 19:429–31. [PubMed: 21481782]
7. Yu H, Pardoll D, Jove R. STATs in cancer inflammation and immunity: a leading role for STAT3. *Nat Rev Cancer.* 2009; 9:798–809. [PubMed: 19851315]
8. Lesina M, Kurkowski MU, Ludes K, Rose-John S, Treiber M, Kloppel G, et al. Stat3/Socs3 activation by IL-6 transsignaling promotes progression of pancreatic intraepithelial neoplasia and development of pancreatic cancer. *Cancer Cell.* 2011; 19:456–69. [PubMed: 21481788]

9. Fukuda A, Wang SC, Morris JPt, Folias AE, Liou A, Kim GE, et al. Stat3 and MMP7 contribute to pancreatic ductal adenocarcinoma initiation and progression. *Cancer Cell*. 2011; 19:441–55. [PubMed: 21481787]
10. Johnston PA, Grandis JR. STAT3 signaling: anticancer strategies and challenges. *Mol Interv*. 2011; 11:18–26. [PubMed: 21441118]
11. Jiang JL, Zhou Q, Yu MK, Ho LS, Chen ZN, Chan HC. The involvement of HAb18G/CD147 in regulation of store-operated calcium entry and metastasis of human hepatoma cells. *J Biol Chem*. 2001; 276:46870–7. [PubMed: 11591720]
12. Xu J, Xu HY, Zhang Q, Song F, Jiang JL, Yang XM, et al. HAb18G/CD147 functions in invasion and metastasis of hepatocellular carcinoma. *Mol Cancer Res*. 2007; 5:605–14. [PubMed: 17579119]
13. Zhao P, Zhang W, Wang SJ, Yu XL, Tang J, Huang W, et al. HAb18G/CD147 promotes cell motility by regulating annexin II-activated RhoA and Rac1 signaling pathways in hepatocellular carcinoma cells. *Hepatology*. 2011; 54:2012–24. [PubMed: 21809360]
14. Chen Y, Zhang H, Gou X, Horikawa Y, Xing J, Chen Z. Upregulation of HAb18G/CD147 in activated human umbilical vein endothelial cells enhances the angiogenesis. *Cancer Lett*. 2009; 278:113–21. [PubMed: 19223118]
15. Tang J, Guo YS, Zhang Y, Yu XL, Li L, Huang W, et al. CD147 induces UPR to inhibit apoptosis and chemosensitivity by increasing the transcription of Bip in hepatocellular carcinoma. *Cell Death Differ*. 2012; 19:1779–90. [PubMed: 22595757]
16. Ke X, Fei F, Chen Y, Xu L, Zhang Z, Huang Q, et al. Hypoxia upregulates CD147 through a combined effect of HIF-1 α and Sp1 to promote glycolysis and tumor progression in epithelial solid tumors. *Carcinogenesis*. 2012; 33:1598–607. [PubMed: 22678117]
17. Li Y, Xu J, Chen L, Zhong WD, Zhang Z, Mi L, et al. HAb18G (CD147), a cancer-associated biomarker and its role in cancer detection. *Histopathology*. 2009; 54:677–87. [PubMed: 19438743]
18. Weidle UH, Scheuer W, Eggle D, Klostermann S, Stockinger H. Cancer-related issues of CD147. *Cancer Genomics Proteomics*. 2010; 7:157–69. [PubMed: 20551248]
19. Chen ZN, Mi L, Xu J, Song F, Zhang Q, Zhang Z, et al. Targeting radioimmunotherapy of hepatocellular carcinoma with iodine (131I) metuximab injection: clinical phase I/II trials. *Int J Radiat Oncol Biol Phys*. 2006; 65:435–44. [PubMed: 16690431]
20. Xu J, Shen ZY, Chen XG, Zhang Q, Bian HJ, Zhu P, et al. A randomized controlled trial of Licartin for preventing hepatoma recurrence after liver transplantation. *Hepatology*. 2007; 45:269–76. [PubMed: 17256759]
21. Wu J, Ru NY, Zhang Y, Li Y, Wei D, Ren Z, et al. HAb18G/CD147 promotes epithelial-mesenchymal transition through TGF- β signaling and is transcriptionally regulated by Slug. *Oncogene*. 2011; 30:4410–27. [PubMed: 21532623]
22. Ke X, Li L, Dong HL, Chen ZN. Acquisition of anoikis resistance through CD147 upregulation: A new mechanism underlying metastasis of hepatocellular carcinoma cells. *Oncol Lett*. 2012; 3:1249–54. [PubMed: 22783427]
23. Ma XK, Wang L, Li Y, Yang XM, Zhao P, Tang H, et al. HAb18G/CD147 cell-cell contacts confer resistance of a HEK293 subpopulation to anoikis in an E-cadherin-dependent manner. *BMC Cell Biol*. 2010; 11:27–40. [PubMed: 20398401]
24. Riethdorf S, Reimers N, Assmann V, Kornfeld JW, Terracciano L, Sauter G, et al. High incidence of EMMPRIN expression in human tumors. *Int J Cancer*. 2006; 119:1800–10. [PubMed: 16721788]
25. Zhang W, Erkan M, Abiatari I, Giese NA, Felix K, Kayed H, et al. Expression of extracellular matrix metalloproteinase inducer (EMMPRIN/CD147) in pancreatic neoplasm and pancreatic stellate cells. *Cancer Biol Ther*. 2007; 6:218–27. [PubMed: 17224648]
26. Tsai WC, Chao YC, Sheu LF, Lin YF, Nieh S, Chen A, et al. EMMPRIN and fascin overexpression associated with clinicopathologic parameters of pancreaticobiliary adenocarcinoma in Chinese people. *APMIS*. 2007; 115:929–38. [PubMed: 17696949]
27. Pan Y, He B, Song G, Bao Q, Tang Z, Tian F, et al. CD147 silencing via RNA interference reduces tumor cell invasion, metastasis and increases chemosensitivity in pancreatic cancer cells. *Oncol Rep*. 2012; 27:2003–9. [PubMed: 22427101]

28. Schneiderhan W, Scheler M, Holzmann KH, Marx M, Gschwend JE, Bucholz M, et al. CD147 silencing inhibits lactate transport and reduces malignant potential of pancreatic cancer cells in vivo and in vitro models. *Gut*. 2009; 58:1391–8. [PubMed: 19505879]
29. Kim H, Zhai G, Liu Z, Samuel S, Shah N, Helman EE, et al. Extracellular matrix metalloproteinase as a novel target for pancreatic cancer therapy. *Anticancer Drugs*. 2011; 22:864–74. [PubMed: 21730821]
30. Kim H, Zhai G, Samuel SL, Rigell CJ, Umphrey HR, Rana S, et al. Dual combination therapy targeting DR5 and EMMPRIN in pancreatic adenocarcinoma. *Mol Cancer Ther*. 2012; 11:405–15. [PubMed: 22203731]
31. Cited; available from: www.oncomine.org.
32. Iacobuzio-Donahue CA, Maitra A, Olsen M, Lowe AW, van Heek NT, Rosty C, et al. Exploration of global gene expression patterns in pancreatic adenocarcinoma using cDNA microarrays. *Am J Pathol*. 2003; 162:1151–62. [PubMed: 12651607]
33. Logsdon CD, Simeone DM, Binkley C, Arumugam T, Greenson JK, Giordano TJ, et al. Molecular profiling of pancreatic adenocarcinoma and chronic pancreatitis identifies multiple genes differentially regulated in pancreatic cancer. *Cancer Res*. 2003; 63:2649–57. [PubMed: 12750293]
34. Pei H, Li L, Fridley BL, Jenkins GD, Kalari KR, Lingle W, et al. FKBP51 affects cancer cell response to chemotherapy by negatively regulating Akt. *Cancer Cell*. 2009; 16:259–66. [PubMed: 19732725]
35. Li M, Zhai Q, Bharadwaj U, Wang H, Li F, Fisher WE, et al. Cyclophilin A is overexpressed in human pancreatic cancer cells and stimulates cell proliferation through CD147. *Cancer*. 2006; 106:2284–94. [PubMed: 16604531]
36. Song F, Zhang X, Ren XB, Zhu P, Xu J, Wang L, et al. Cyclophilin A (CyPA) induces chemotaxis independent of its peptidylprolyl cis-trans isomerase activity: direct binding between CyPA and the ectodomain of CD147. *J Biol Chem*. 2011; 286:8197–203. [PubMed: 21245143]
37. Bauer K, Kretzschmar AK, Cvijic H, Blumert C, Loffler D, Brocke-Heidrich K, et al. Cyclophilins contribute to Stat3 signaling and survival of multiple myeloma cells. *Oncogene*. 2009; 28:2784–95. [PubMed: 19503092]
38. Yurchenko V, Constant S, Eisenmesser E, Bukrinsky M. Cyclophilin-CD147 interactions: a new target for anti-inflammatory therapeutics. *Clin Exp Immunol*. 2010; 160:305–17. [PubMed: 20345978]
39. Bourguignon LY, Peyrollier K, Xia W, Gilad E. Hyaluronan-CD44 interaction activates stem cell marker Nanog, Stat-3-mediated MDR1 gene expression, and ankyrin-regulated multidrug efflux in breast and ovarian tumor cells. *J Biol Chem*. 2008; 283:17635–51. [PubMed: 18441325]
40. Slomiany MG, Grass GD, Robertson AD, Yang XY, Maria BL, Beeson C, et al. Hyaluronan, CD44, and emmprin regulate lactate efflux and membrane localization of monocarboxylate transporters in human breast carcinoma cells. *Cancer Res*. 2009; 69:1293–301. [PubMed: 19176383]
41. Hao J, Chen H, Madigan MC, Cozzi PJ, Beretov J, Xiao W, et al. Co-expression of CD147 (EMMPRIN), CD44v3–10, MDR1 and monocarboxylate transporters is associated with prostate cancer drug resistance and progression. *Br J Cancer*. 2010; 103:1008–18. [PubMed: 20736947]
42. Lin L, Hutzen B, Zuo M, Ball S, Deangelis S, Foust E, et al. Novel STAT3 phosphorylation inhibitors exhibit potent growth-suppressive activity in pancreatic and breast cancer cells. *Cancer Res*. 2010; 70:2445–54. [PubMed: 20215512]
43. Liao CG, Kong LM, Song F, Xing JL, Wang LX, Sun ZJ, et al. Characterization of basigin isoforms and the inhibitory function of basigin-3 in human hepatocellular carcinoma proliferation and invasion. *Mol Cell Biol*. 2011; 31:2591–604. [PubMed: 21536654]
44. Ji Q, Hao X, Zhang M, Tang W, Yang M, Li L, et al. MicroRNA miR-34 inhibits human pancreatic cancer tumor-initiating cells. *PLoS One*. 2009; 4:e6816. [PubMed: 19714243]
45. Lian J, Wu X, He F, Karnak D, Tang W, Meng Y, et al. A natural BH3 mimetic induces autophagy in apoptosis-resistant prostate cancer via modulating Bcl-2-Beclin1 interaction at endoplasmic reticulum. *Cell Death Differ*. 2011; 18:60–71. [PubMed: 20577262]

46. Shah N, Zhai G, Knowles JA, Stockard CR, Grizzle WE, Fineberg N, et al. (18)F-FDG PET/CT imaging detects therapy efficacy of anti-EMMPRIN antibody and gemcitabine in orthotopic pancreatic tumor xenografts. *Mol Imaging Biol.* 2012; 14:237–44. [PubMed: 21494920]
47. Zhang X, Liu P, Zhang B, Wang A, Yang M. Role of STAT3 decoy oligodeoxynucleotides on cell invasion and chemosensitivity in human epithelial ovarian cancer cells. *Cancer Genet Cytogenet.* 2010; 197:46–53. [PubMed: 20113836]
48. Zoller M. CD44: can a cancer-initiating cell profit from an abundantly expressed molecule? *Nat Rev Cancer.* 2011; 11:254–67. [PubMed: 21390059]
49. Su YJ, Lai HM, Chang YW, Chen GY, Lee JL. Direct reprogramming of stem cell properties in colon cancer cells by CD44. *Embo J.* 2011; 30:3186–99. [PubMed: 21701559]
50. Marotta LL, Almendro V, Marusyk A, Shipitsin M, Schemme J, Walker SR, et al. The JAK2/STAT3 signaling pathway is required for growth of CD44(+)CD24(–) stem cell-like breast cancer cells in human tumors. *J Clin Invest.* 2011; 121:2723–35. [PubMed: 21633165]
51. Slomiany MG, Dai L, Tolliver LB, Grass GD, Zeng Y, Toole BP. Inhibition of Functional Hyaluronan-CD44 Interactions in CD133-positive Primary Human Ovarian Carcinoma Cells by Small Hyaluronan Oligosaccharides. *Clin Cancer Res.* 2009; 15:7593–601. [PubMed: 19996211]

Translational Relevance

The failure of conventional chemotherapeutic agents on survival of patients with pancreatic cancer highlights an urgent need for novel treatment strategies. STAT3 plays a critical role in pancreatic cancer initiation and progression and represents a novel therapeutic target. However, STAT3 occupies a point of convergence for many signaling pathways; blockade of existed upstream signaling to STAT3 activation are not sufficient to abrogate STAT3 activation. This study identified HAb18G/CD147 as a novel upstream activator in STAT3-mediated pancreatic tumor development by forming signaling complex with CD44s. Furthermore, we showed that pancreatic cancer patients with high co-expression of HAb18G/CD147-CD44s-STAT3 had poor prognosis. This information is valuable for a better understanding of the relationship between inflammation and pancreatic cancer initiation and progression induced by STAT3. Our results also suggest HAb18G/CD147 as a novel therapeutic target for highly aggressive pancreatic cancer and as a surrogate marker in clinical trials of molecular therapy targeting STAT3.

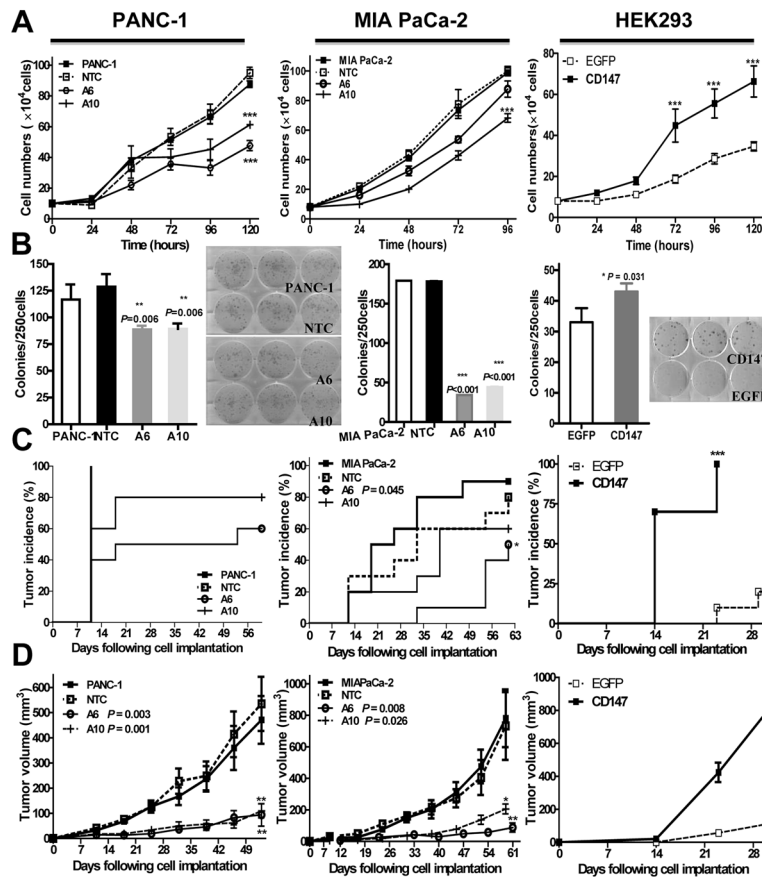


Figure 1. HAB18G/CD147 promotes *in vitro* cellular and clonogenic growth and *in vivo* pancreatic tumor formation

(A) *In vitro* cell growth assay in HAB18G/CD147 knock-down PANC-1 (left) and MIA PaCa-2 (middle) cells, as well as HAB18G/CD147 knock-in HEK293 (right) cells by stably transfected with pLKO.1 CD147 shRNA A6, A10 or CD147 cDNA. (B) *In vitro* clonogenic growth assay by counting formed colonies. (C) Tumor incidence in xenograft mouse models with HAB18G/CD147 knock-down PANC-1 (left) and MIA PaCa-2 (middle) cells, as well as HAB18G/CD147 knock-in HEK293 cells (right). (D) Tumor volume at different time point in xenograft mouse models ($n=10$) with HAB18G/CD147 knock-down PANC-1 (left) and MIA PaCa-2 (middle) cells, as well as HAB18G/CD147 knock-in HEK293 cells (right).

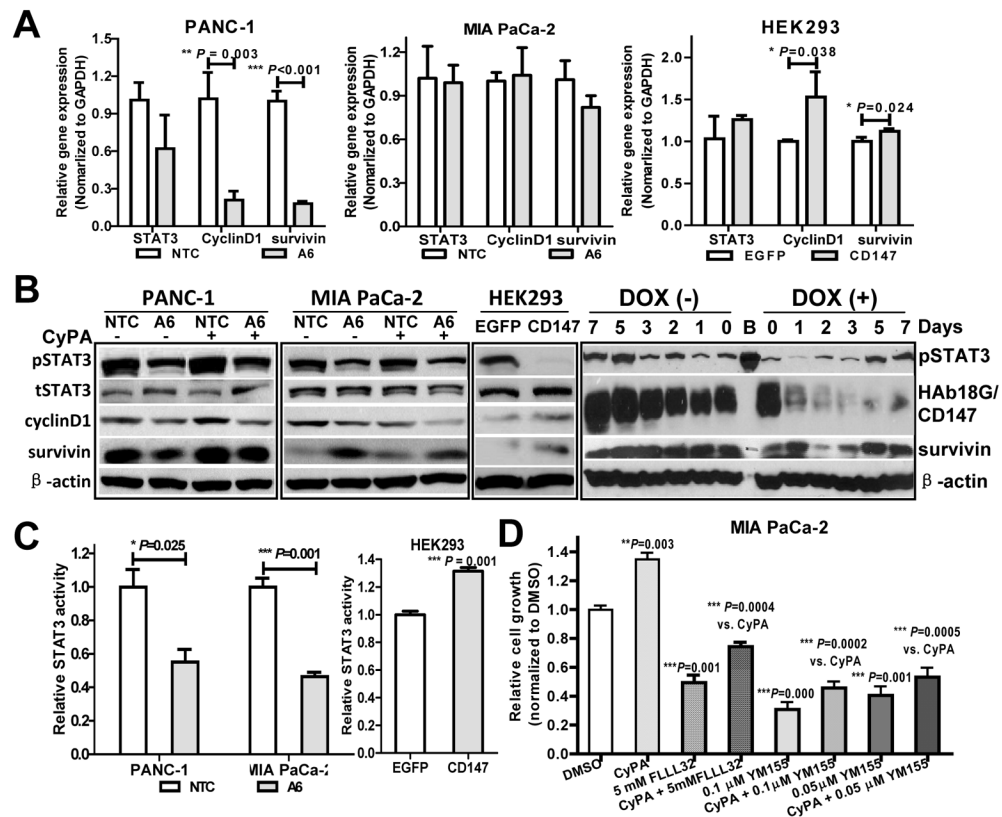


Figure 2. CyPA-HAb18G/CD147 promotes pSTAT3 mediated cell growth

(A) STAT3/cyclinD1/survivin mRNA levels in HAb18G/CD147 knock-down or knock-in cells. (B) pSTAT3, tSTAT3, cyclinD1 and survivin protein levels in serum-starved HAb18G/CD147 knockdown or knock-in cells treated with or without 100 nmol/L CypA for 30 min (left), and in pTRIPZ inducible knock-down cells with or without DOX treatment at indicated time points (right). (C) STAT3 reporter assay in HAb18G/CD147 knock-down or knock-in cells. (D) Cell growth assay in MIA PaCa-2 cells treated with or without STAT3 inhibitor FLLL32 (5 μ mol/L), survivin inhibitor YM155 (0.05–0.1 μ mol/L) and/or CyPA (100 nmol/L).

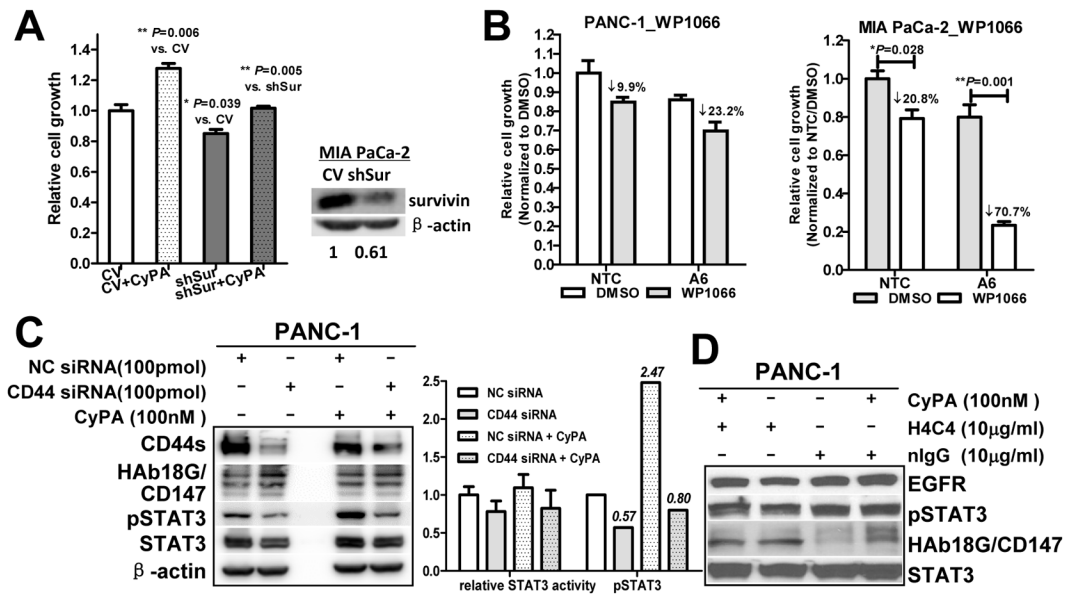


Figure 3. HAB18G/CD147 activates pSTAT3 signaling via CD44s

(A) Cell growth assay in survivin shRNA or empty vector (EV) transfected MIA PaCa-2 cells with or without 100 nmol/L CyPA treatment. Efficiency of the knock-down was confirmed by immunoblot analysis (right). (B) Cell growth assay in HAB18G/CD147 knock-down cells after the exposure to STAT3 inhibitor WP1066. (C) HAB18G/CD147, CD44s, pSTAT3 and STAT3 protein expression (left) and STAT3 transcription activity (right) in CD44s siRNA knock-down PANC-1 cells with or without CyPA treatment. Negative siRNA was included as control. (D) HAB18G/CD147, EGFR, pSTAT3 and STAT3 protein expression in PANC-1 cells with or without H4C4 or/and CyPA treatment.

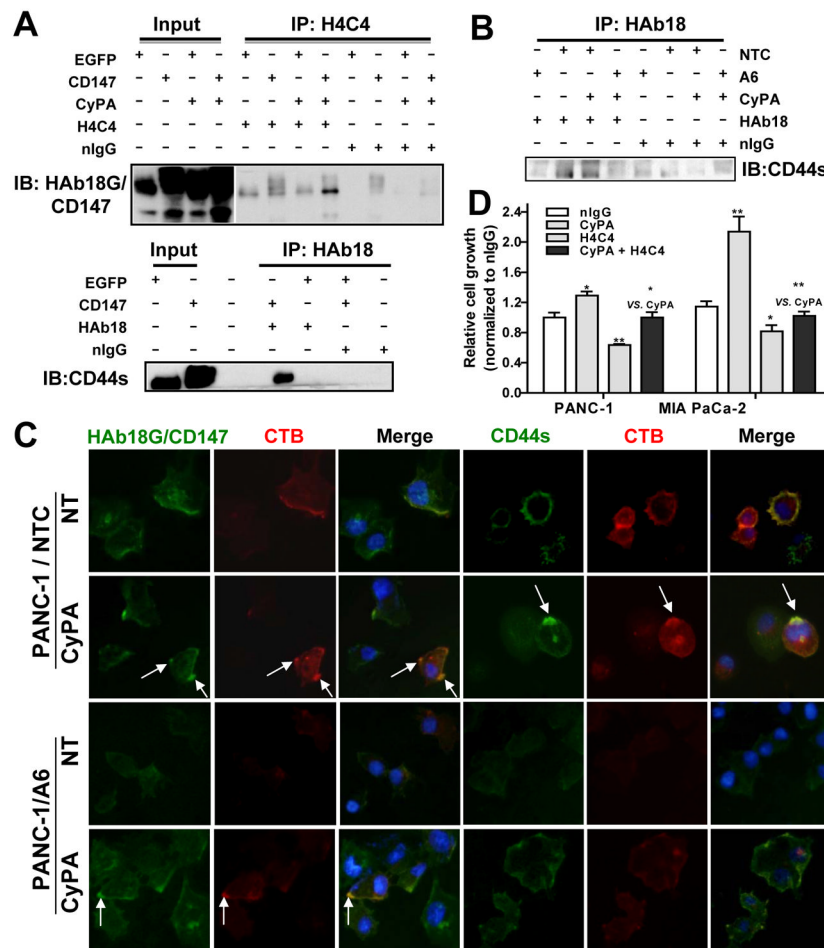


Figure 4. HAb18G/CD147 and CD44s are co-expressed and associated in pancreatic cancer cells
(A) Immunoprecipitation analysis of the HAb18G/CD147 and CD44s in HAb18G/CD147 knock-in HEK293 cells with or without CyPA treatment. Normal mouse nIgG was used as a control antibody. **(B)** Immunoprecipitation analysis of the HAb18G/CD147 and CD44s in HAb18G/CD147 knock-down MIA PaCa-2 cells with or without 100 nmol/L CyPA treatment. **(C)** Co-immunolabeling of HAb18G/CD147 (green) or CD44s (green) with lipid raft marker CTB (red) in HAb18G/CD147 knock-down PANC-1 cells. Magnification: 400 \times . Arrows indicated co-localization of HAb18G/CD147 or CD44s with CTB in lipid rafts. **(D)** Cell growth assay in PANC-1 and MIA PaCa-2 cells with CD44s blocking antibody H4C4 (10 μ g/mL) and/or CypA (100 nmol/L).

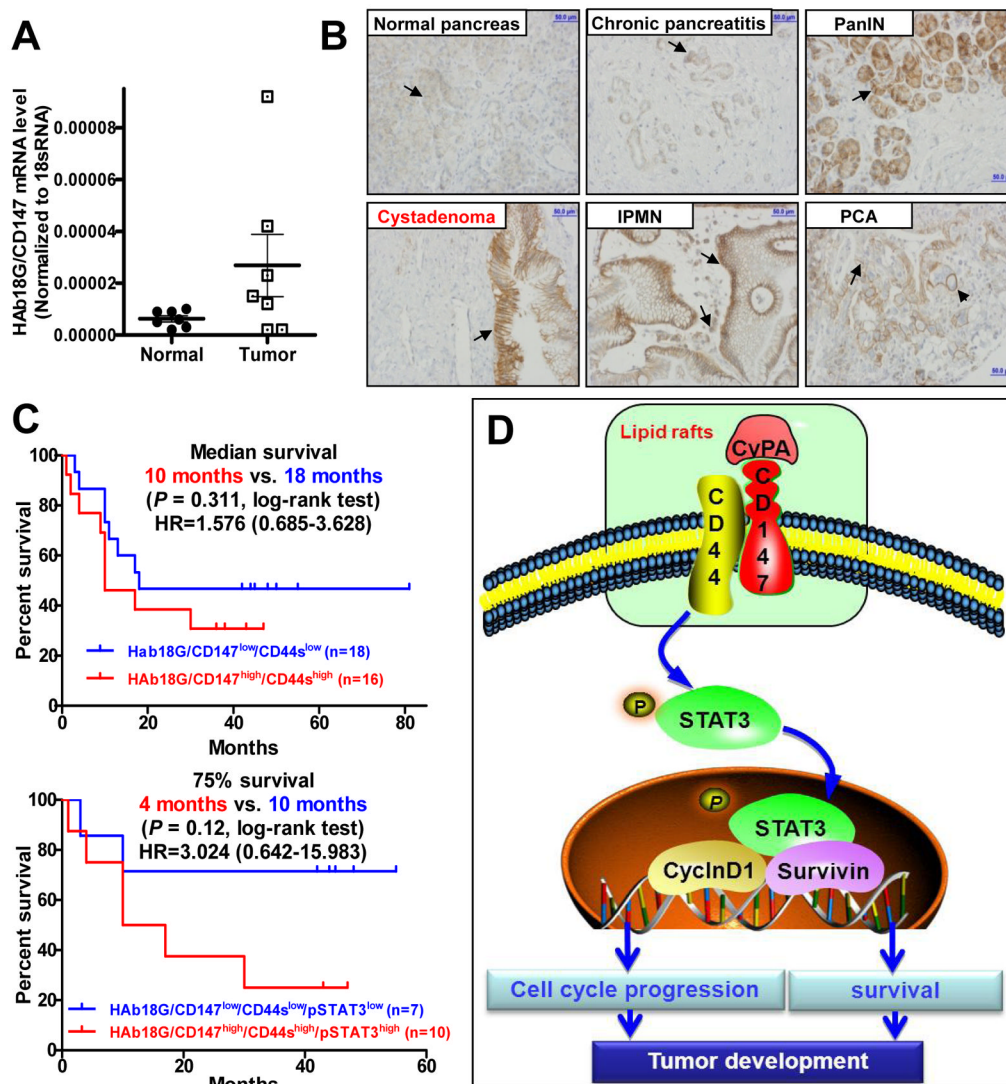


Figure 5. HAB18G/CD147-CD44s-pSTAT3 co-expression in pancreatic cancer is clinically correlated

(A) HAB18G/CD147 mRNA levels in 7 pairs of pancreatic adenocarcinoma and the adjacent normal tissues. Levels were normalized against 18sRNA levels. (B) HAB18G/CD147 protein levels in normal pancreas, chronic pancreatitis, pancreatic intraepithelial neoplasia (PanIN), cystadenoma (CYSTADEMA), intraductal papillary mucinous neoplasm (IPMN), and pancreatic adenocarcinoma (PDCA). Representative morphology of HAB18G/CD147 and CD44s immunostaining in pancreatic cancer tissues. (C) Kaplan-Meier analysis of overall survival for 34 patients based on HAB18G/CD147 and CD44s scores by immunohistochemistry staining (up); and Kaplan-Meier analysis of overall survival for 17 patients based on immunohistochemistry staining scores of HAB18G/CD147, CD44s and pSTAT3 (down). (D) A proposed working model for HAB18G/CD147 interaction with CD44s signaling during pSTAT3-activated pancreatic tumor development.

Table 1

HAb18G/CD147 expression in pancreatic tissues

	HAb18G/CD147 expression levels ^a				P value ^b
	0	1	2	3	
Normal	26.4% (14/53)	26.4% (14/53)	24.5% (13/53)	22.6% (12/53)	/
Pancreatitis	14.3% (1/7)	28.6% (2/7)	42.9% (3/7)	14.3% (1/7)	0.967
Preneoplasms	12% (3/25)	20% (5/25)	12% (3/25)	56% (14/25)	0.004
PanIn	0	50% (1/2)	0	50% (1/2)	N
CYSTADEMA	16.7% (1/6)	16.7% (1/6)	16.7% (1/6)	50% (3/6)	N
IPMN	11.8% (2/17)	17.6% (3/17)	11.8% (2/17)	58.8% (10/17)	0.006
PDA	7.4% (8/108)	18.5% (20/108)	18.5% (20/108)	55.6% (60/108)	0.000

^a HAb18G/CD147 expression levels are scored as: 0 (no staining), 1 (light staining), 2 (intermediate staining) and 3 (intense staining).

^b Estimated by χ^2 test as compared with normal tissues by dividing into low and high expression group. Low expression group (LEG) are cases with staining intensity scores of 0-2; High expression group (HEG) are cases with staining intensity scores of 3. N, not detected.

Table 2

Spearman's correlation coefficients for the correlation among expression of HAb18G/CD147, STAT3 and CD44s

Gene expression	HAb18G/CD147	Nuclear pSTAT3	Cytoplasm pSTAT3	CD44s
HAb18G/CD147	—	-0.035	-0.098	0.496 [‡]
Nuclear pSTAT3	-0.035	—	0.415 [‡]	0.165 [*]
Cytoplasm pSTAT3	-0.098	0.415 [‡]	—	0.019
CD44s	0.496 [‡]	0.165 [*]	0.019	—

[‡]P < 0.001,

[#]P < 0.01, and

^{*}P < 0.05.